Hindawi Publishing Corporation
Journal of Chemistry
Volume 2015, Article ID 796459, 15 pages
http://dx.doi.org/10.1155/2015/796459

Research Article

Influence of Filler from a Renewable Resource and Silane Coupling Agent on the Properties of Epoxidized Natural Rubber Vulcanizates

Wiphawadee Pongdong,[1] Charoen Nakason,[2] Claudia Kummerlöwe,[3] and Norbert Vennemann[3]

[1]*Department of Rubber Technology and Polymer Science, Faculty of Science and Technology, Prince of Songkla University, Pattani Campus, Pattani 94000, Thailand*
[2]*Faculty of Science and Industrial Technology, Prince of Songkla University, Surat Thani Campus, Surat Thani 84000, Thailand*
[3]*Faculty of Engineering and Computer Science, Osnabrück University of Applied Sciences, Albrechtstrasse 30, 49076 Osnabrück, Germany*

Correspondence should be addressed to Norbert Vennemann; n.vennemann@hs-osnabrueck.de

Received 25 November 2014; Revised 8 February 2015; Accepted 10 February 2015

Academic Editor: Cengiz Soykan

Rice husk ash (RHA) was used as a reinforcing filler in epoxidized natural rubber (ENR) with various loading levels (0, 10, 20, and 30 phr), and silica filled ENR was also studied for comparison. The effects of RHA content on cure characteristics, mechanical properties, dynamic mechanical properties, and thermoelastic behavior of the filled ENR composites were investigated. It was found that the incorporation of RHA significantly affected the cure characteristics and mechanical properties. That is, the incorporation of RHA caused faster curing reactions and increased Young's modulus and tensile strength relative to the unfilled compound. This might be attributed to the metal oxide impurities in RHA that enhance the crosslinking reactions, thus increasing the crosslink density. Further improvements in the curing behavior and the mechanical properties of the filled composites were achieved by *in situ* silanization with bis(triethoxysilylpropyl) tetrasulfide (Si69). It was found that the rubber-filler interactions reinforced the composites. This was indicated by the decreased damping characteristic (tan δ) and the other changes in the mechanical properties. Furthermore, the ENR composites with Si69 had improved filler dispersion. Temperature scanning stress relaxation (TSSR) results suggest that the metal oxide impurities in RHA promote degradation of the polymer network at elevated temperatures.

1. Introduction

Natural rubber (NR) is a natural biosynthesis polymer that has been widely used for numerous applications because of its excellent mechanical and elastic properties. However, the application of NR is limited due to some drawbacks. That is, NR is highly susceptible to degradation because of the double bonds in the main chain. Several ways to modify natural rubber molecules have been proposed to overcome these problems, including the incorporation of some functional groups onto the NR molecules. Epoxidation has been one of the most popular alternatives, modifying the molecular structure of NR by adding epoxide groups onto the NR molecules. Epoxidized natural rubber (ENR) has improved heat and oil resistance and low air permeability and viscosity. However, ENR with low epoxide content still retains the strain crystallization tendency of natural rubber. Furthermore, the polarity of ENR increases with the degree of epoxidation [1].

Reinforcement of rubber and polymer materials by particulate fillers is a common practice for improving the service properties and reducing the production cost. The most important fillers are the conventional synthetic fillers carbon black and silica. Production of these conventional fillers is highly energy-consuming. Therefore, alternative fillers from renewable resources are of considerable interest, improving

the overall sustainability of filled rubber production. Rice husk ash (RHA) is obtained by burning the agricultural rice husk waste, and it mainly consists of amorphous silica and residual carbon black from combustion. The amount of silica in RHA varies between 55 and 97 wt%, depending on the combustion conditions. Rice is the staple food of over half of the world's population, and about one-fifth of the world's population is engaged in rice cultivation. The global rice production was about 750 million tons in 2013, and the husks contribute about one-fifth by weight of the harvested and dried crops. The husks contain about 20% silica. Therefore, silica containing rice husk ash is generated in excess of 30 million tons per year [2]. Some prior research has assessed the properties of silica ash, to obtain an in-depth understanding of its behavior, and has specifically tried to identify suitable modifications to improve its performance as filler. The potential of RHA as a filler material for polymer composites has been investigated with various polymers such as polyethylene (PE) [3, 4], polypropylene (PP) [5], [styrene butadiene rubber (SBR)] + [linear low-density polyethylene (LLDPE)] blends, [6] and polyurethane (PU) [7]. In RHA/rubber composites, enhanced curing rate was observed with increased RHA loading levels in EPDM, while contrary trends were observed in silica composites [8]. In a comparative study of the cure characteristics, processability, and mechanical properties of NR/EPDM blends filled with RHA, silica, or carbon black, the RHA filling gave the best resilience properties [9]. It was also found that the incorporation of RHA in natural rubber resulted in lowered Mooney viscosity and shortened cure time and improved hardness but decreased tensile strength and tear strength [10].

Influences of the two types of RHA, namely, black rice husk ash (BRHA, silica content of 54%) and white rice husk ash (WRHA, silica content of 95%), on the mechanical properties of epoxidized natural rubber with 50% mole epoxide (i.e., ENR-50) were investigated in [11]. It was found that the WRHA exhibits overall superior vulcanizate properties to those with BRHA. The effects of RHA on the properties of unmodified natural rubber, compared with ENR-50 composites, were also reported [12]. The results indicated that the NR composites exhibited longer scorch and cure times with higher tensile strength and elongation at break but lower tensile modulus than that of the ENR-50 composites.

To improve the mechanical properties of polymer composites, filler surfaces have been treated with various types of coupling agents. However, the most commonly used coupling agent in rubber compounds is bis(triethoxysilylpropyl) tetrasulfide (Si69). The effects of Si69 on the properties of RHA filled natural rubber (NR) were investigated in [13]. No improvement was found in the mechanical properties of RHA filled vulcanizates with the silane coupling agent (Si69). This was presumably caused by the lack of silanol groups on the RHA surfaces. The effects of coupling agent (Si69) and a chemical treatment of RHA filled natural rubber were also investigated in [14]. In this case, the silane coupling agent marginally improved the performance of rubber vulcanizates.

In this work, RHA filled ENR-25 composites with various filler contents were prepared. Cure characteristics, tensile properties, dynamical mechanical thermal analysis (DMTA), crosslink density, thermoelastic properties, and relaxation behavior of RHA filled ENR-25 vulcanizates were investigated. Furthermore, an *in situ* modification of silica with the silane coupling agent in the ENR-25 compounds was investigated. The silane coupling agent was directly added to the internal mixer during the mixing of RHA and ENR-25. The silanization reaction might take place under the mixing conditions. A conventional commercial precipitated silica was also used as the filler, to prepare composites for comparisons between alternative fillers.

2. Experimental

2.1. Materials. Epoxidized natural rubber (ENR) with 25 mol% epoxide was prepared in house by using preparation method described elsewhere [15]. The high ammonia (HA) concentrated natural rubber latex, used as raw material in the preparation of ENR, was manufactured by Yala Latex Industry Co., Ltd., (Yala, Thailand). The ENR with a 25 mol% level of epoxide groups was prepared via performic epoxidation, by reacting NR latex with *in situ* performic acid generated from a reaction of formic acid (94% purity, manufactured by Riedel De Haen, (Seelze, Germany)) and hydrogen peroxide (50 wt%, manufactured by Riedel De Haen (Seelze, Germany)). Characterization of the prepared ENR was also performed by ^{1}H-NMR, Mooney viscometer, and DSC. Results confirmed that it was the ENR with 26 mol% epoxide having 96.6 (ML 1 + 4), 100°C, and Tg of −42.65°C. The RHA filler was supplied by Thunyakit Nakhon Pathom Rice Mill Co., Ltd., (Nakhon Pathom, Thailand). The silica, Ultrasil 7000 GR, was manufactured by Evonik Industries, (Essen, Germany). The bis(triethoxysilylpropyl) tetrasulfide (Si69) was manufactured by Evonik Industries (Essen, Germany) and was used as a silane coupling agent. The sulfur used as a curing agent was manufactured by Pergan GmbH (Bocholt, Germany). The N-tert-butyl-2 benzothiazolesulfenamide (Santocure, TBBS) used as an accelerator was manufactured by Rhein Chemie Rheinau GmbH, (Mannheim, Germany). The 1,3-diphenylguanidine (DPG) used as an secondary accelerator was manufactured by Evonik Industries (Essen, Germany). The zinc oxide used as a cure activator was manufactured by Lanxess (Leverkusen, Germany). The other cure activator, namely, stearic acid, was manufactured by Unichema International B.V. (Gouda, Netherlands).

2.2. Characterization of RHA. RHA was obtained from burning of the rice husks during the rice manufacturing process. When the burning is incomplete the result is carbonized rice husks (CRH). Typically, the particles of RHA or CRH are reduced in size by milling and further by grinding and are sieved through 120-mesh screen. The powder of this type that we obtained was placed in aluminum crucibles and put in a muffle furnace (Thermolyne 6000 furnace, Barnstead International, Dubuque, USA), and a heat treatment was performed at 700°C for 6 h [16]. This caused reduction of the carbonaceous material and increased the relative content of silicon oxide. The chemical composition and the functional

Table 1: Compounding formulation.

Ingredients	Gum	RHA_{10}	RHA_{10}-Si69	RHA_{20}	RHA_{20}-Si69	RHA_{30}	RHA_{30}-Si69	S_{30}	S_{30}-Si69
ENR-25	100	100	100	100	100	100	100	100	100
ZnO	5	5	5	5	5	5	5	5	5
Stearic acid	1	1	1	1	1	1	1	1	1
Wingstay-L	1	1	1	1	1	1	1	1	1
TBBS	0.6	0.6	0.6	0.6	0.6	0.6	0.6	0.6	0.6
Sulfur	2	2	2	2	2	2	2	2	2
RHA	—	10	10	20	20	30	30	—	—
Silica[a]	—	—	—	—	—	—	—	30	30
TESPT	—	—	0.01	—	0.02	—	0.03	—	2.4
DPG	—	—	0.003	—	0.005	—	0.008	—	0.3

[a]Silica (Ultrasil 7000 GR).

groups of the RHA were characterized by X-ray fluorescence spectrometer (XRF) and by Fourier transform infrared spectroscopy (FT-IR). Also, the particle size distribution of RHA was analyzed by a particle size analyzer (Beckman Coulter LS 230, Vernon Hills, Illinois, USA). The surface area of RHA was also determined by the Brunauer-Emmett-Teller (BET) method. The structure of RHA particles was visualized by scanning electron microscopy (SEM) (JSM-6510LA, Jeol Ltd., Akishima, Japan). The density was measured by an ultrapycnometer. Finally, the pH of the RHA was determined using the procedure described in ASTM D1512.

2.3. Mixing and Vulcanization. The rubber compounds were prepared using the compounding formulation shown in Table 1. The Haake Rheocord 600 laboratory internal mixer (Thermo Electron Corporation, Karlsruhe, Germany) with a fill factor of 0.7 was used to mix the rubber and other chemicals at 80°C at a rotor speed of 40 rpm. The ENR-25 was first masticated and compounded with various contents of RHA (10, 20, and 30 phr, labeled as RHA_{10}, RHA_{20}, and RHA_{30}, resp.). Furthermore, the compounds without filler (gum ENR-25), as well as ENR-25 compounded with 30 phr of silica (S_{30}), were prepared as control samples for comparisons. The bis(triethoxysilylpropyl) tetrasulfide coupling agent (Si69) was also mixed with RHA or silica (labels RHA_{10}-Si69, RHA_{20}-Si69, RHA_{30}-Si69, and S_{30}-Si69). It is noted that the contents of Si69 and DPG used in this formulation were fixed based on the specific surface areas of the fillers according to [17]

$$\begin{aligned} \text{Si69 content } (\text{phr}) &= 0.00053 \times Q \times CTAB, \\ \text{DPG content } (\text{phr}) &= 0.00012 \times Q \times CTAB, \end{aligned} \tag{1}$$

where Q is the filler content (phr) and $CTAB$ is the specific surface area of silica or RHA (m^2/g).

Cure characteristics of the rubber compounds were then studied by using a rotorless rheometer, D-MDR 3000 (Montech, Werkstoffprüfmaschinen GmbH, Buchen, Germany) at 160°C for 30 min. The compounds were then vulcanized in an electrically heated plate press (Polystat 200 T type, Schwabenthan, Wustermark, Germany) under 70-bar pressure at 160°C. The rubber vulcanizates were eventually conditioned for 24 h before testing and characterization.

2.4. Mechanical Properties. Mechanical properties in terms of tensile strength and modulus were determined using a universal tensile testing machine (Hounsfield Tensometer, model H 10KS, Hounsfield Test Equipment Co., Ltd., Surrey, UK). The machine was operated at room temperature, with an extension speed of 500 mm/min, according to the procedures described in ASTM D412. Dumbbell-shaped specimens were die-cut from the vulcanized rubber sheets using ASTM die type C.

2.5. Dynamic Mechanical Properties. Dynamic mechanical properties of the rubber vulcanizates were measured using an advanced rheometric expansion system rheometer (model ARES-RDA W/FCO, TA Instruments Ltd., New Castle, The United States). The instrument was operated in the torsion mode at a frequency of 1.0 Hz and at dynamic strain amplitude of 0.5%. The temperatures range was set from −60 to 20°C, with a heating rate of 2°C/min.

2.6. Crosslink Density. Apparent crosslink densities of the rubber vulcanizates were determined using a swelling method. Rectangular 10 × 10 × 2 mm test pieces were used. The samples were weighted before immersing into toluene and were left in the dark under ambient conditions for seven days. The swollen samples were then removed and excess liquid on the specimen surfaces was removed by blotting with filter paper. The specimens were then dried in an oven at 60°C until constant weight [18]. The final weights of the samples were then compared with their original weights before immersion into toluene. The apparent crosslink density was calculated by using the Flory-Rehner equation [19]:

$$\nu = \frac{-\left(\ln\left(1-\phi_\rho\right)+\phi_\rho+\chi\phi_\rho^2\right)}{V_1\left(\phi_\rho^{1/3}-\phi_{\rho/2}\right)}, \tag{2}$$

where ν is the crosslink density (mol/m^3), ϕ_ρ is the volume fraction of rubber in a swollen network, V_1 refers to the molar volume of toluene, and χ is the Flory-Huggins interaction

Table 2: Physical properties of rice husk ash (RHA) and silica.

Properties	RHA	Silica
Mean particle size (μm)	3.83	0.018
Surface area (m^2/g)	0.91	173
Density (g/cm^3)	2.18	2.10
pH	9.20	6.50

parameter between toluene and rubber, where a value of 0.4 was used for χ according to the literature [20].

It is noted that the volume fraction of filler had to be subtracted in the calculation of the volume fraction of rubber in a swollen network (ϕ_ρ). Thus, the volume fraction of rubber in a swollen network was determined by

$$\phi_\rho = \frac{1}{\left(1 + \left(\left(m - m_d\right)/m_d\right)\right) \cdot \left(\rho_p/\rho_s\right)}, \quad (3)$$

where m is the mass of the swollen sample, m_d is the mass after drying of the sample, ρ_p is density of the polymer, and ρ_s is density of the solvent [21].

2.7. Temperature Scanning Stress Relaxation. The thermoelastic behavior of each rubber vulcanizate was determined by using a TSSR meter (Brabender, Duisburg, Germany) operated at a constant tensile strain of 50%. A dumbbell-shaped specimen (type 5A, ISO 527) was placed in an electrically heated test chamber, regulated to the initial 23°C temperature, for 2 h. This is to allow the decay of short-time relaxation processes. The sample was then heated with a constant heating rate of 2°C/min until the stress relaxation was complete or the sample ruptured. From the resulting stress-temperature curve or force-temperature curve, the nonisothermal relaxation modulus, $E(T)$, can be obtained specifically for the used constant heating rate ν. The relaxation spectrum, $H(T)$, was obtained by differentiating $E(T)$ with respect to temperature, T, according to [21–23]

$$H(T) = -T\left[\frac{dE(T)}{dT}\right]_{\nu=\text{const}}. \quad (4)$$

2.8. Morphological Properties. Microstructures of the rubber vulcanizates were studied by scanning electron microscopy (SEM) (model JSM-6510LA, Jeol Ltd., Akishima, Japan). The sample surfaces were first prepared by cryogenic fracturing and were then coated with a thin layer of gold under vacuum conditions, before characterization by SEM.

3. Results and Discussion

3.1. Characteristics of RHA and Silica. The physical properties in terms of particle size, surface area, density, and pH of RHA and silica are summarized in Table 2. It can be seen that the mean particle size of RHA is considerably larger than that of the silica, Ultrasil 7000 GR. That is, the mass-average particle size based on the particle size distribution curve of RHA (Figure 1) is approximately 3.83 μm, while the commercial silica shows very small particles with a mean particle size of about 0.018 μm (Table 2). Also, the BET surface area of RHA is considerably lower than that of the silica particles. Furthermore, it is seen that pH is higher for RHA than for the silica. This might be attributed to the presence of impurities, in particular metal oxides, as shown in Table 3. The topography of RHA particles characterized by SEM technique is shown in Figure 2. It is seen that the RHA particles are irregular in shape with smooth surface.

Table 3: Chemical compositions of RHA.

Chemical composition	Concentration (%)
Silicon dioxide (SiO_2)	91.04
Potassium oxide (K_2O)	3.70
Phosphorus pentoxide (P_2O_5)	1.36
Calcium oxide (CaO)	1.96
Magnesium oxide (MgO)	0.45
Alumina (Al_2O_3)	0.52
Iron oxide (Fe_2O_3)	0.60
Manganese oxide (MnO)	0.32
Barium oxide (BaO)	0.03
Lead oxide (PbO)	0.05
Rubidium oxide (Rb_2O)	0.02

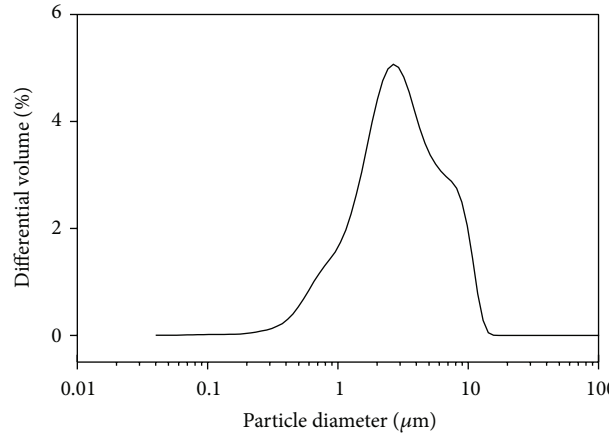

Figure 1: Particle size distribution curve of RHA.

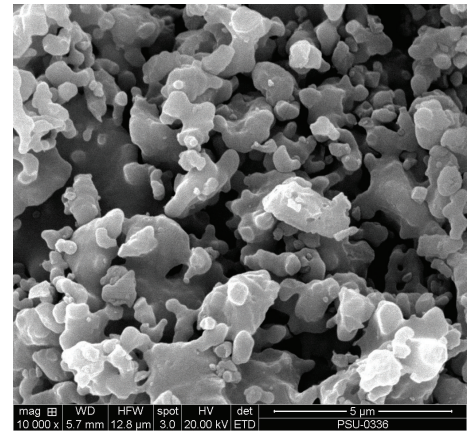

Figure 2: SEM micrograph of RHA particle.

Table 4: Cure characteristics of gum and filled ENR-25 vulcanizates with various RHA contents or 30 phr of silica, with and without silane coupling agent (Si69).

Sample	Min. torque (M_L, dN m)	Max. torque (M_H, dN m)	Delta torque (M_H–M_L, dN m)	Scorch time (t_{s2}, min)	Cure time (t_{90}, min)
Gum	1.14	5.6	4.46	3.84	8.16
RHA_{10}	1.44	5.73	4.29	3.10	4.61
RHA_{20}	1.55	6.15	4.60	2.70	4.28
RHA_{30}	1.82	7.71	5.89	2.40	4.59
RHA_{10}-Si69	1.16	5.97	4.81	1.48	2.89
RHA_{20}-Si69	1.23	6.68	5.45	1.27	2.69
RHA_{30}-Si69	1.36	8.17	6.81	1.03	2.73
S_{30}	5.13	14.45	9.32	3.67	19.54
S_{30}-Si69	4.61	16.72	12.11	2.68	9.28

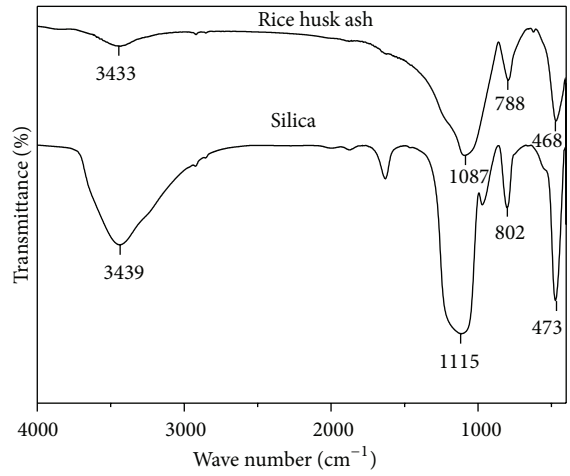

Figure 3: FTIR spectra of RHA and silica.

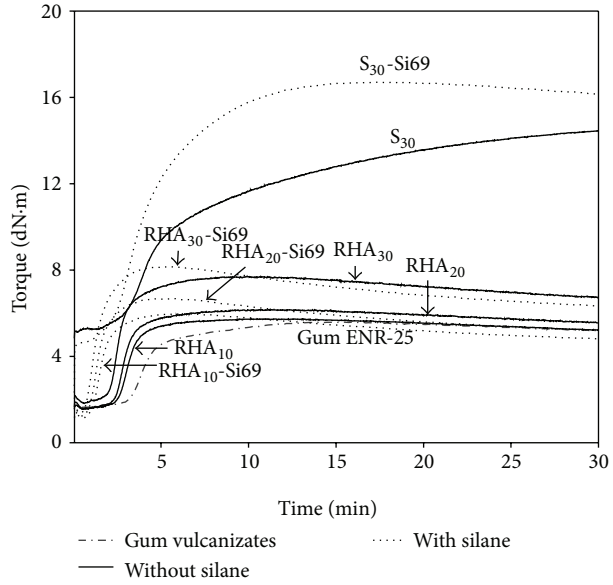

Figure 4: Cure curves of gum and filled ENR-25 vulcanizates with various contents of RHA and 30 phr silica with and without silane coupling agent (Si69).

Figure 3 shows the infrared spectra of RHA and silica. It is seen that the absorption peak at a wave number of 3433 cm^{-1}, which is assigned to the stretching vibration of silanol groups and the hydrogen bonds between water and adjacent (vicinal) silanols (–OH), is observed in both spectra. Also, the absorption peak at the wave number 1087 cm^{-1}, which is assigned to the asymmetrical stretching vibration of Si–O–Si, is observed. Furthermore, the absorption peaks at wave numbers 788 and 468 cm^{-1}, which represent the characteristic bands of amorphous silica, are also observed in both samples [13, 24]. It is therefore concluded that the RHA and silica show similar infrared spectra indicating the characteristics of silica. Also, in the spectrum of RHA, the characteristic peak of hydrocarbon is not observed. This confirms that burning in the muffle furnace at 700°C for 6 h completely eliminated the carbon content in the RHA.

3.2. Cure Characteristics. Figure 4 shows the curing curves of the gum and the filled ENR-25 compounds, with various contents of RHA and with 30 phr of silica, with and without silane coupling agent (Si69). Plateau curing curves were observed for the gum and the RHA filled compounds. However, the reversion phenomenon with decreasing torque was observed for the filled ENR-25 compounds with RHA-Si69. This is attributed to the restructuring and changing crosslink structures of rubber vulcanizates after the maximum vulcanization [25]. Also, the breakdown of monosulfidic and ether linkages contributes to the reversion in the ENR networks [26]. On the other hand, the silica filled ENR-25 compound (S_{30}) exhibits marching curing with increasing torque, with cure retardation. This might be attributed to reactions between the silica and the zinc oxide accelerator, which subsequently lowers the ability to form zinc complex intermediates and slows down the vulcanization process. In addition, the incorporation of the silane coupling agent enhanced the cure characteristics by forming filler-silane-ENR linkages. That is, all silane treated compounds exhibit short cure times (t_{90}) and scorch times (t_{s2}) and high torque differences or delta torques, as shown in Table 4.

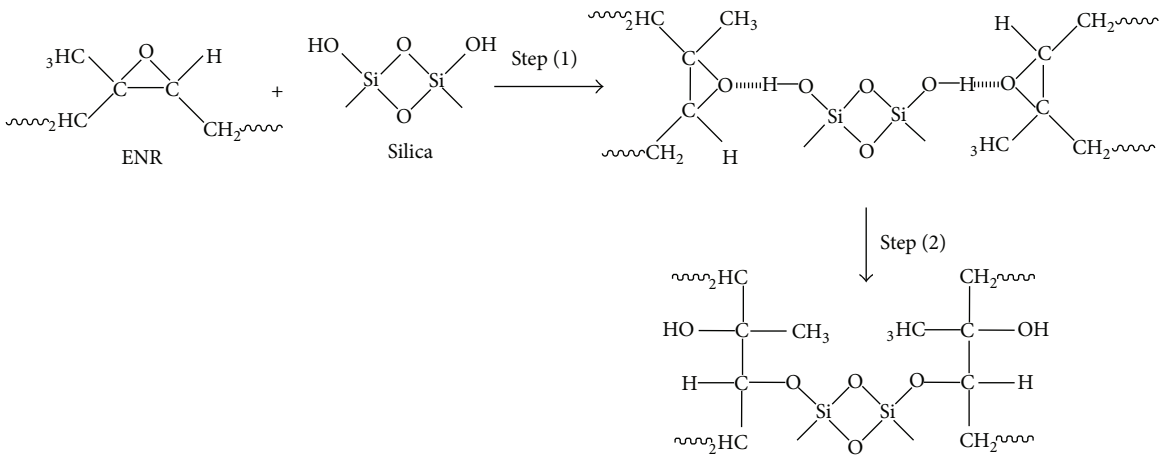

Scheme 1: Possible chemical interaction between ENR and silica.

In Table 4, it is also clear that scorch and cure times were shortened by increasing the content of RHA. This might be attributed to the presence of metal oxides in the RHA, which enhances crosslinking reactions and increases cure rates of the rubber compounds [9–14]. However, at equal filler loading levels of 30 phr, the RHA exhibited shorter scorch and cure times than the silica. The most probable factor to account for this observation is the specific surface area, with low specific surface allowing less hydroxyl groups on the RHA surfaces [27, 28]. This reduces the cure retardation by the adsorption of curatives. In Table 4, the M_H and M_L increased with the loading level of RHA. That is, addition of filler usually increases the modulus and significantly reduces the chain mobility of rubber macromolecules. The relatively high M_L and cure torque of silica filled ENR compound with 30 phr indicates its high stiffness caused by the silica particulates. This stiffness also restricts the chain mobility due to obstruction by the filler particles and probably by the strong interaction between silica and the ENR matrix. Further, the expected increase in modulus is partly due to the inclusion of rigid filler particles in the soft matrix, while another contribution arises from the filler-rubber interactions. The latter effect relates to the smaller particle size and correspondingly high specific surface area of silica (Table 2). In the ENR compounds with silane coupling agent, all filled rubber vulcanizates exhibit low M_L but high M_H and torque difference (i.e., delta torque). This may be attributed to the involvement of silane molecules in vulcanization, resulting in chemical linkages being established between the silane and the filler together with the ENR-25 matrix. The vulcanizate properties are enhanced by the silane coupling agent through the polymer-polymer and polymer-filler interactions. It is noted that an increase in delta torque indicates an increase in crosslink density. Also, shortened scorch and cure times were observed in the filled ENR-25 with the silane coupling agent. This might be due to the presence of sulfur atoms in the silane coupling agent (Figure 5). Otherwise the functional groups that link the coupling agent to the rubber molecules form double bonds, which are activated by the addition of an active sulfur compound or by the generation of a radical moiety

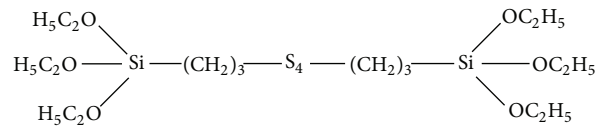

Figure 5: Chemical structure of silane coupling agent Si69.

in order to have simultaneous crosslinking of rubber and the coupling agent molecules with comparable reaction rate during the curing. The silane coupling agent also increases the amount of sulfur in the rubber compounds, which may cause crosslinking reactions and hence shorten the scorch and cure times.

3.3. Mechanical Properties. The effects of the various filler loadings with alternative fillers and the use of silane coupling agent on the mechanical properties of ENR-25 vulcanizates in terms of Young's modulus, tensile strength, and elongation at break are shown in Figures 6 to 8. In Figure 6, it is seen that the Young's modulus increased with RHA content. The incorporation of RHA particles restricts the mobility of rubber molecular chains and hence increases material stiffness. This result agrees with the increase of delta torque in Table 4. It is also seen that the filled ENR vulcanizates exhibited higher Young's moduli and tensile strengths than the gum vulcanizate. Furthermore, these properties increased slightly with the loading level of RHA. This may be attributed to the dilution effect together with the reinforcement, because of chemical interactions between the RHA particles and the ENR matrix. It is noted that the RHA surfaces carry hydroxyl groups and other oxygen compounds (Table 2). These can interact with the epoxide groups in ENR molecules, and a potential reaction is shown in Scheme 1. That is, the silanol groups on the silica surfaces can interact with the epoxide rings in ENR molecules, during mixing and/or vulcanizing. Also, chemical linkages form from silanol groups reacting with the ring opening products of ENR, possibly with the reaction model shown in Figure 9(a). In Figures 6 and 7, it is also seen that the silane coupling agent in RHA increased

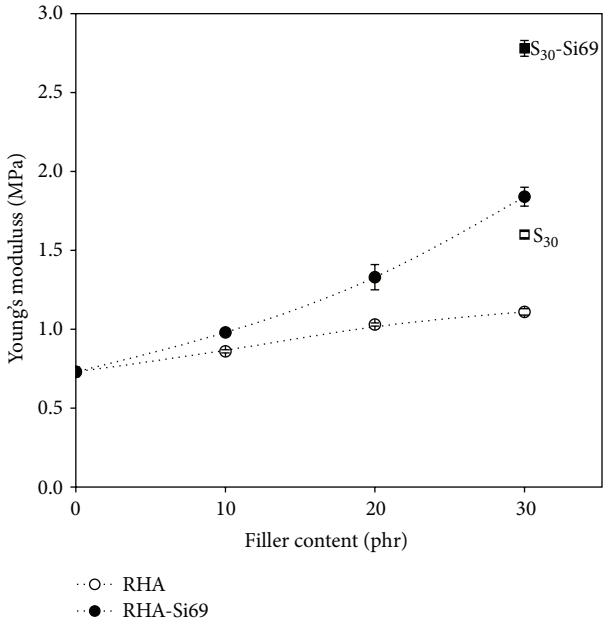

Figure 6: Young's modulus of gum and filled ENR-25 vulcanizates with various RHA contents and 30 phr of silica with and without silane coupling agent (Si69).

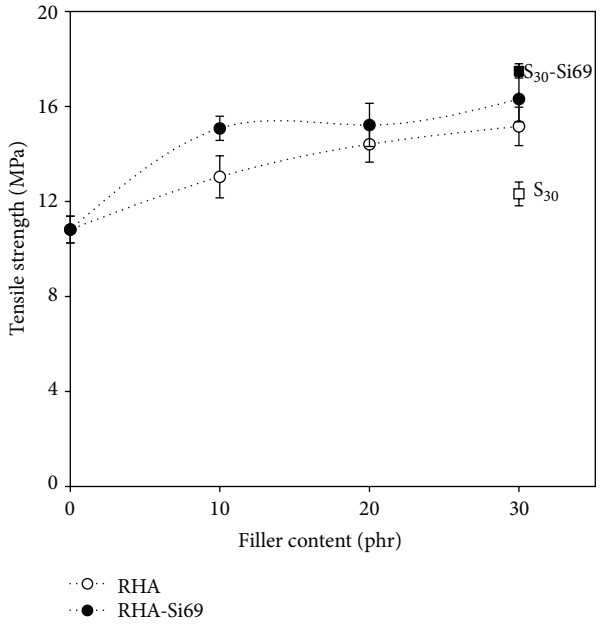

Figure 7: Tensile strength of gum and filled ENR-25 vulcanizates with various RHA contents and 30 phr of silica with and without silane coupling agent (Si69).

Young's modulus and tensile strength of the filled ENR-25 vulcanizates. This might be due to an increased crosslink density caused by the new linkages of silica-Si69-ENR-25, as schematically shown in Figure 9(b). It is also seen that the Young's modulus (Figure 6) and tensile strength (Figure 7) of silica filled ENR-25 vulcanizates with silane coupling agent were higher than those of the RHA filled vulcanizates. This might be attributed to the high specific surface of silica particles, which allows extensive chemical interactions between filler and rubber, thus enhancing polymer-filler interaction.

In Figures 7 and 8, it is also seen that increasing the content of RHA increased the tensile strength but decreased the elongation at break of the RHA filled ENR-25 vulcanizates. This is due to the RHA particles lowering chain mobility of rubber molecules, together with the increased chemical interactions between the RHA particles and the ENR matrix, with a high reinforcing effect. Furthermore, the incorporation of silane coupling agent increased the tensile strength but decreased the elongation at break. This might be due to the surfaces of RHA providing hydroxyl groups and other oxygen compounds (Table 3), which may form hydrogen bonds with the organosilane coupling agent and the epoxide groups in ENR molecules. In Figure 8, it is also seen that the silica filled ENR-25 vulcanizate showed lower elongation at break than that of the RHA filled ENR-25 composite. This might be due to the high polarity of silica that may cause poor filler distribution and increase filler-filler interactions. This is corroborated by the large silica agglomerates observed in the SEM micrograph of Figure 14(d). It is therefore concluded that the rubber vulcanizate with silane coupling agent showed high mechanical properties in terms

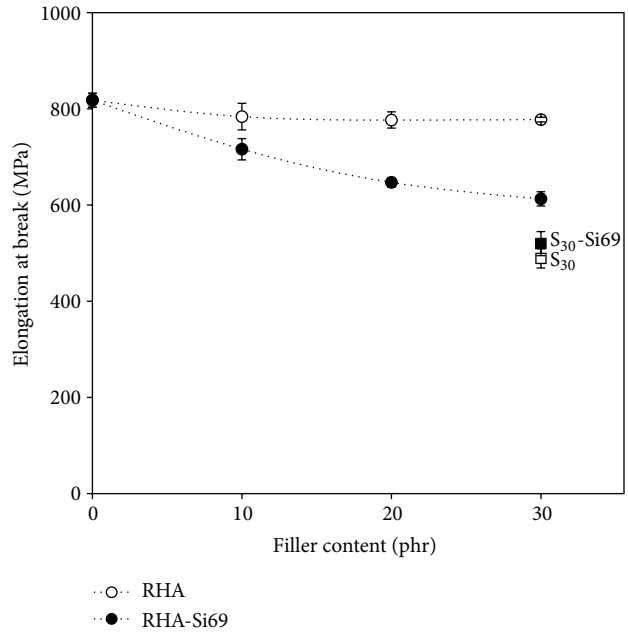

Figure 8: Elongation at break of gum and filled ENR-25 vulcanizates with various RHA contents and 30 phr of silica with and without silane coupling agent (Si69).

of Young's modules and tensile strength but low elongation at break. That is, the silane coupling agent might contribute to good filler dispersion in the elastomeric matrix and to improved adhesion between the two phases. Typically, the coupling agents are bifunctional molecules (Figure 5), which are capable of establishing molecular bridges at the interface

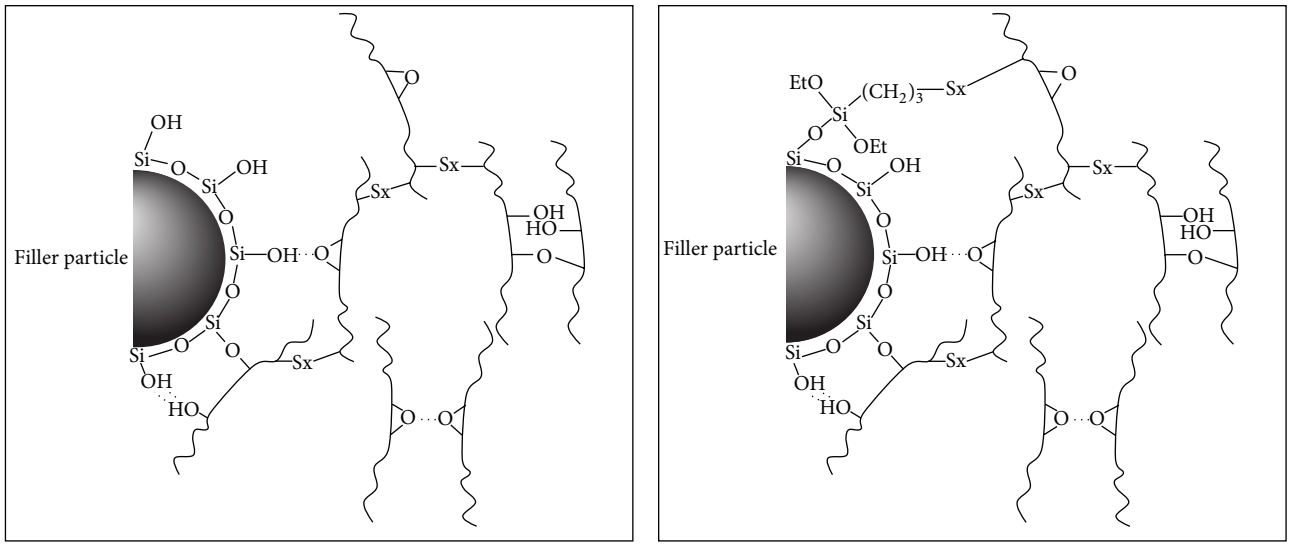

Figure 9: The proposed reaction models for RHA or silica dispersed in ENR-25 matrix (a) without silanization, (b) with silane coupling agent (Si69).

Table 5: Storage moduli at 20°C, loss moduli, and maximum damping factor of gum and filled ENR-25 vulcanizates with 30 phr of RHA or silica, with and without silane coupling agent (Si69).

Sample	Storage modulus G' (MPa)	Loss modulus G'' ($\times 10^5$) (MPa)	Maximum damping factor, $\tan \delta_{max}$
Gum	746.96	2.87	2.77
RHA_{30}	841.64	3.22	2.69
RHA_{30}-Si69	1428.10	3.91	1.96
S_{30}	2927.50	3.25	1.34
S_{30}-Si69	3017.50	3.58	1.41

between the polymer matrix and filler surface, as illustrated in Figure 9(b). Hence, they enhance the rubber-filler adhesion, improve reinforcement effects, and give superior mechanical properties.

3.4. Dynamic Properties. It is well recognized that the storage modulus of a particulate filled polymer composite is influenced by the effective interfacial interaction between the inorganic filler particles and the polymer matrix. In general, a stronger interfacial interaction between the matrix and the filler gives a superior storage modulus of the composite [29]. Dynamic mechanical thermal analysis (DMTA) was exploited to characterize the RHA and silica filled ENR-25 vulcanizates. Figure 10 shows the storage modulus (G'), the loss modulus (G''), and the loss tangent of gum ENR-25 vulcanizates and filled ENR-25 with 30 phr of RHA or silica, with and without silane Si69. In Figure 10(a), it is seen that in the glassy region at temperatures below −55°C the changes in G' were small. That is, the modulus-temperature curves are plateaus. It is also seen that the various types of rubber vulcanizates had the following rank order by storage modulus: gum vulcanizate < RHA filled ENR-25 < RHA filled ENR-25 with Si69 < silica filled ENR-25 < silica filled ENR-25 with Si69 (Table 5). Therefore, the incorporation of RHA or silica in ENR-25 increased the modulus from the gum vulcanizates. This is due to interactions between the silanol groups in silica and the polar functional groups in ENR molecules (Figure 9(a)). Also, the addition of Si69 increased the reinforcement effects of RHA or silica fillers in the vulcanizates (in RHA_{30}-Si69 and S_{30}-Si69). This is simply due to the reactions between the silanol groups of silica, the epoxide groups in ENR, and the organosilane (Figure 9(b)). Therefore, the incorporation of Si69 increased the rubber-filler interactions and consequently enhanced the storage modulus [30]. It is noted that the silica filled ENR-25 vulcanizates, with and without Si69, show higher moduli than the RHA filled vulcanizates. This might be due to the more restricted molecular mobility, due to the greater interactions between the silica and the rubber matrix. In Figure 10(a), it is also seen that increasing the temperature caused an abrupt drop in the storage modulus, before the transition and the rubbery regions. In these regions, it is seen that the storage modulus increased with filler. This could be explained by the higher stiffness of the filled rubber vulcanizates and the hydrodynamic effects associated with

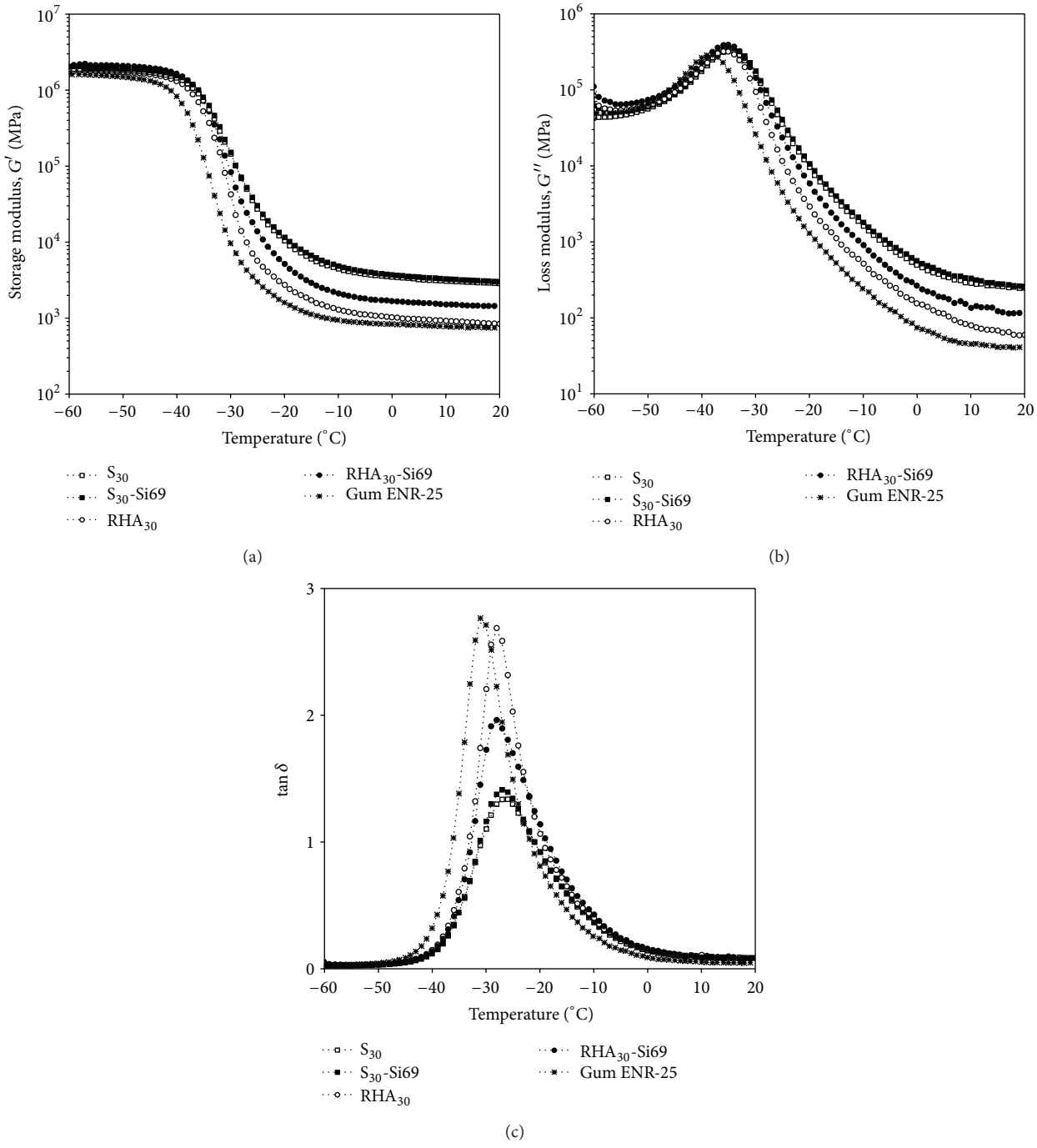

Figure 10: (a) Storage modulus, (b) loss modulus, and (c) tan δ as a function of temperature of ENR-25 gum and filled vulcanizates with 30 phr of RHA and silica with and without silane coupling agent (Si69).

the strong interactions between filler and rubber molecules. Also, the highest modulus of RHA filled ENR-25 vulcanizates was found with Si69. This might be due to increased chemical rubber-filler interactions.

In Figure 10(b), it is clear that the gum vulcanizate shows the lowest loss modulus, which might be related to the mobility of the rubber molecular chains [30]. It is also seen that loss modulus peaks were comparatively broad for the filled ENR-25 samples RHA_{30}, RHA_{30}-Si69, S_{30}, and S_{30}-Si69. This might be due to an increased energy absorption caused by the fillers. Other reasons might be the chemical interactions in RHA_{30}-Si69 and S_{30}-Si69, together with the interactions between ENR-25 and RHA or silica particles, which restrict molecular mobility.

The ratio of loss modulus to storage modulus is referred to as the internal damping or the loss tangent (tan δ) and is an

indicator characterizing the dynamic behavior of materials. The storage moduli at 20°C (G'), the maximum loss moduli (G''), and the variation of maximum damping factor are shown in Table 5 and in Figure 10(c). It is seen that the gum vulcanizates show the lowest storage modulus and loss modulus but the highest tan δ values in the glass transition region. This indicates a large degree of mobility and hence good damping characteristics and elastomeric properties. Tanδ relates to the impact resistance and damping of a material, which mainly depend on the nature of the matrix, the filler, and their interface. Furthermore, there is frictional damping due to slippage in the unbound regions at the interface of filler and matrix, or interfacial delamination, and energy is dissipated by crack propagation in the matrix; all of these phenomena relate to the damping properties [29]. The damping peak usually occurs in the glass transition region and is associated with the movement of side groups or low molecular-weight units within the rubber molecules. Therefore, a high maximum of the damping peak or the damping factor (tan δ_{max}) or the peak area indicates high molecular mobility, as observed in the ENR-25 gum vulcanizates (Figure 10(c)). In Table 5, it is clear that the gum vulcanizate shows the highest tan δ_{max}, indicating good mobility and damping characteristics. In Figure 10(c), it is also seen that the incorporation of fillers in the ENR-25 vulcanizates decreased the damping characteristics and gave low and broad damping peaks. This might be attributed to the filler retarding the mobility of rubber chains, restricting the segmental motions of the rubber molecules, by the strong filler-rubber interactions. It is also seen that the RHA_{30}-Si69 showed a lower tan δ_{max} than the one without silane coupling agent. This may be attributed to the silane coupling agent improving the filler-rubber interaction. The decreased value of tan δ_{max} suggests a relatively high filler-rubber interaction [31]. The temperature at which the tan δ peak appears is an estimated value of the glass transition temperature (T_g) and the height of the peak can be used to quantitate the reinforcement of rubber. In Figure 10(c), slight differences are seen in the T_g for the gum vulcanizate and the RHA filled ENR-25 with or without silane coupling agent (Si69). That is, the filler shifted the T_g for filled rubber vulcanizates, especially in the RHA filled ENR-25 with silane coupling agent, towards higher temperatures. This might be attributed to the crosslinking that restricts the mobility of the polymer chains, or other increased rubber-filler interactions. It is also seen that the silica filled ENR-25 vulcanizate showed higher storage (G') and loss moduli (G'') but lower maximum damping factor (tan δ_{max}) than the RHA filled ENR-25 vulcanizates, with or without silane coupling agent, and the same goes for the unfilled gums. This might be due to the high polarity of silica, with high polymer-filler and filler-filler interactions. Hence the silica gives high reinforcing effects and strongly restricts the segmental motions of rubber.

3.5. Crosslink Density. Figure 11 and Table 6 show the apparent crosslink densities based on the Flory-Rehner equation (equation (2)), for the gum and the filled ENR-25 vulcanizates with various contents of RHA or silica, with and without Si69. It can be seen that the apparent crosslink density increased with the RHA content. In general, the crosslink density is the number of linkages between rubber molecules per unit volume. In the filled rubber vulcanizates, the filler particles act as additional multifunctional crosslinking sites interacting physically and/or chemically with the rubber molecules. That is, the rubber-filler linkages contribute effectively increasing the crosslink density. Obviously, the number of linkages increased with RHA or silica loading. The addition of Si69 also increased the crosslink density, especially at the high 20 and 30 phr filler concentrations. The increases in apparent crosslink density may be caused by two different crosslinking reactions, namely, the interaction of hydroxyl groups on silica ash surfaces with the polar functional groups in ENR molecules (Figure 9(a)) and the crosslinking of SiO_2-Si69-rubber (Figure 9(b)) [32]. It is also seen

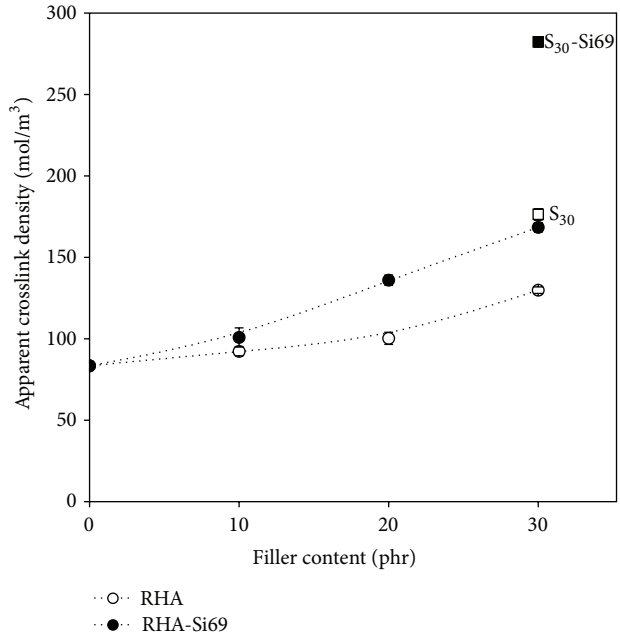

Figure 11: Apparent crosslink densities of gum and filled ENR-25 vulcanizates with various RHA contents and 30 phr of silica with and without silane coupling agent (Si69).

Table 6: Crosslink densities of gum and filled ENR-25 vulcanizates with various RHA contents and 30 phr of silica with and without silane coupling agent (Si69).

Sample	Crosslink density (mol/m^3)
Gum	83.36 ± 1.41
RHA_{10}	92.33 ± 2.74
RHA_{20}	100.27 ± 3.72
RHA_{30}	129.87 ± 1.95
RHA_{10}-Si69	100.92 ± 5.73
RHA_{20}-Si69	136.01 ± 3.16
RHA_{30}-Si69	168.45 ± 2.88
S_{30}	176.37 ± 3.50
S_{30}-Si69	282.25 ± 2.80

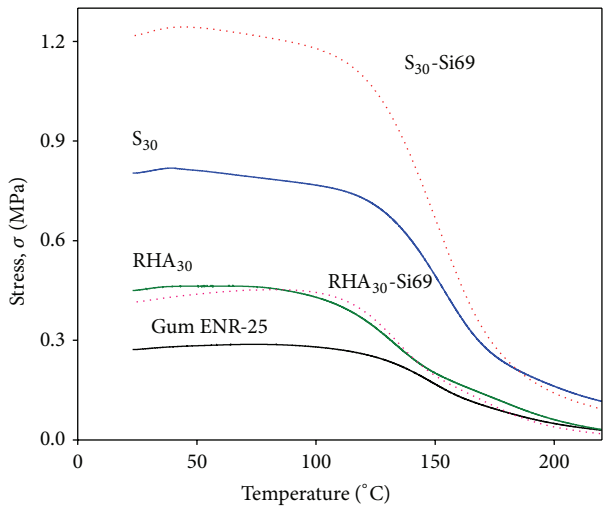

FIGURE 12: Stress as a function of temperature of gum and filled ENR-25 vulcanizates with 30 phr of RHA and silica with and without silane coupling agent (Si69).

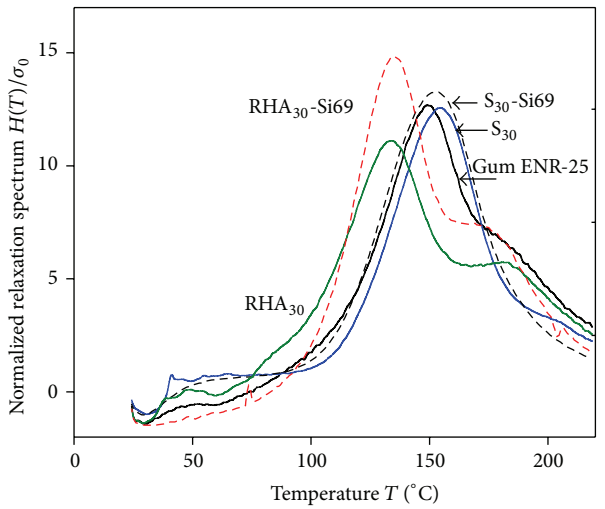

FIGURE 13: Normalized relaxation spectrums as a function of temperature of gum and filled ENR-25 vulcanizates with 30 phr of RHA and silica with and without silane coupling agent (Si69).

that the apparent crosslink density correlates well with the mechanical properties, that is, modulus and tensile strength (Figures 6 and 7), and the dynamic mechanical properties (Figure 10). In Figure 11, it is also seen that the silica filled ENR-25 vulcanizate had a higher crosslink density with Si69 than without it and surpassed all the RHA filled ENR-25 vulcanizates. This might be due to the high specific surface of silica, with hydroxyl groups on the surfaces giving chemical interactions. The higher amount of chemically bound rubber content significantly improves filler dispersion with less filler-filler interaction and higher reinforcement [33].

3.6. Temperature Scanning Stress Relaxation. The thermoelastic and relaxation behavior of the ENR-25 vulcanizates were characterized by the temperature scanning stress relaxation (TSSR) technique, from an initial elongation of $\varepsilon 0 = 50\%$ and with a heating rate of 2°C/min. This technique has been used to examine the relaxation behavior in relation to crosslink density, for polymer blends as well as for filled rubber composites [21–23, 34]. Generally, it can be expected that the stress at a constant extension initially increases with temperature, due to the entropic elasticity of rubber, and at higher temperatures the physical and chemical relaxations will counteract this trend. In particular, the debonding of bound rubber from the filler surfaces, the cleavage of sulfur bridges, and the scission of polymer main chains contribute to relaxation.

Figure 12 shows the stress as a function of the temperature for gum and filled ENR-25 vulcanizates with 30 phr of RHA or silica, with and without silane coupling agent (Si69). It can be seen that initially the stress slightly increased with temperature, as expected because of the entropy effect. Stress relaxation, that is, the decrease of stress, occurred at higher temperatures with the stress approaching zero. Severe stress relaxation is caused by thermooxidative chain scission and by degradation of crosslinks, in particular cleavage of the sulfur bridges, which occurs at temperatures above 130°C. In contrast, the physically induced relaxation of polymer-filler interactions occurs at lower temperatures. Also, the adsorbed polymer layer or glassy layer with polymer segments restricts the polymer chain mobility at the filler surface and reduces reinforcement of the vulcanizates. At high temperatures, the weak physical interactions between filler particles and polymer segments can be overcome by thermal energy, and the polymer segments are released from the filler surface if an external stress is applied. This is evidenced by the decreasing trend of stress with increasing temperature that depends on the amount of desorbed polymer segments. This is evident in the silica filled vulcanizates and can also be seen in the RHA filled vulcanizates. In Figure 12, it is also seen that the initial stress σ_0 increases with incorporation of filler. This could be explained by the higher stiffness of the filled rubber vulcanizate and by the hydrodynamic effects associated with strong interactions between filler and rubber molecules. Therefore, the incorporation of RHA or silica in ENR-25 increased the initial stress relative to the gum vulcanizates. Moreover, with silica filler the initial stress was higher with silane coupling agent Si69 than without it. This is attributed to the high crosslink density caused by chemical filler-rubber interactions, or to the strong polymer-filler interactions. This correlates well with the trends in the mechanical properties, namely, tensile strength and Young's modulus, and with the crosslink density. However, the addition of RHA leads to different results with respect to the initial stress. The RHA filled ENR-25 had slightly higher initial stress without silane coupling agent Si69. The small amount of silane coupling agent used, together with the low specific surface area of RHA that reduced the availability of hydroxyl groups, may have caused the low initial stresses.

Figure 13 shows the relaxation spectra $H(T)$ calculated using (4). To facilitate comparisons the spectra were normalized to show $H(T)$ relative to the initial stress. It can be

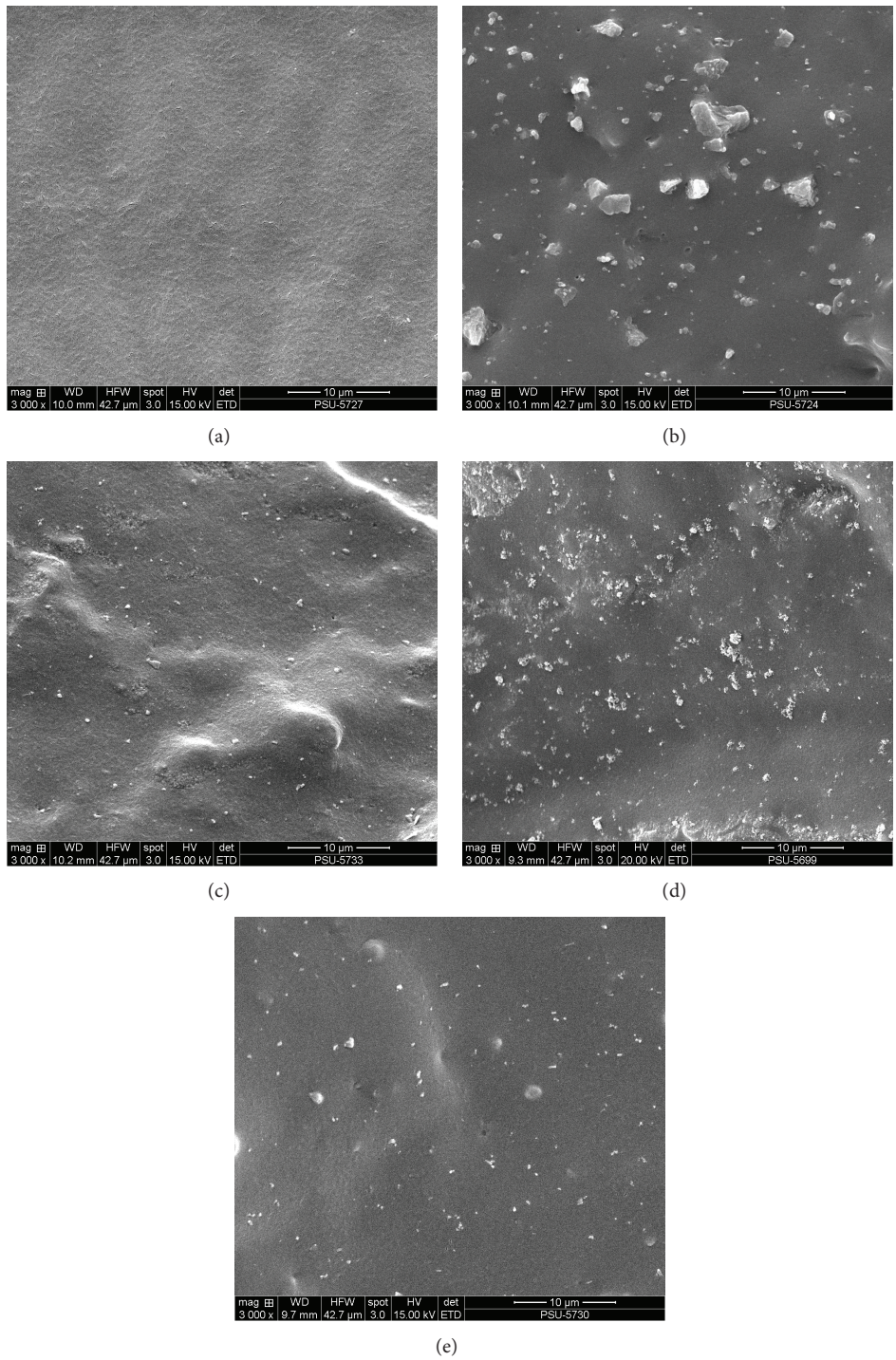

Figure 14: SEM micrographs of gum and filled ENR-25 vulcanizates with 30 phr of RHA and silica with and without silane coupling agent (Si69): (a) gum vulcanizates; (b) RHA_{30}; (c) RHA_{30}-Si69; (d) S_{30}; (e) S_{30}-Si69.

seen that the relaxation spectrum of the pure ENR-25 gum vulcanizate exhibits a dominant peak at about 150°C and a broadening shoulder peak at about 170 to 190°C. These peaks are attributed to polymer network degradation caused by the cleavage of sulfur linkages and scission of the polymer main chains. That is, the dominant peak at 150°C corresponds to the cleavage of long polysulfidic bonds (–C–Sx–C–), whereas the shoulder peak at about 170 to 190°C represents the dissociation of short monosulfidic and disulfidic linkages (–C–S–C–) and the scission of main polymer chains, which might occur at this higher temperature due to the higher binding energies [35]. This reflects the higher binding energy of the –C–S–C– and –C–C–, compared to the polysulfidic linkages (–C–Sx–C–); the thermal stability of the composite network

correlates with the highest peak temperature obtained from the relaxation spectra. Therefore, the peaks of the relaxation spectrum reflect thermal stability. The relaxation spectra of silica filled vulcanizates differ significantly from the unfilled vulcanizates in that the peak at 170–190°C almost vanishes. However, the peak at 150°C is more or less unaffected by the addition of silica. Also, a broad small peak is recognizable in the relaxation spectra of the silica filled vulcanizates at the lower temperatures from 30 to 90°C. This is attributed to the release of polymer segments of the glassy layer, or of adsorbed polymer layer from the filler surface [22].

In Figure 13, it is seen that addition of RHA leads to a different relaxation behavior. That is, the peaks are shifted towards lower temperatures. This is presumably caused by the metal impurities in RHA, which may promote degradation of the polymer network. Furthermore, the silanization of RHA resulted in new chemical linkages between the polymer segments and the RHA particles. This is obviously indicated by the peak in the temperatures from 30 to 60°C, which reflects the debonding of the glassy layer or adsorbed polymer layer at the RHA interface. The RHA filled ENR-25 vulcanizates without Si69 have a recognizable small peak, while with silanization that peak vanishes. Furthermore, the peak is much smaller than for the silica filled ENR-25 vulcanizate, because of the difference in specific surface areas.

3.7. Scanning Electron Microscopy. Figure 14 shows SEM micrographs of cryogenically fractured surfaces of the gum as well as the RHA and silica filled ENR-25 vulcanizates. It is seen that the gum vulcanizate had a smooth fractured surface with some white ZnO particles, in Figure 14(a). However, the fractured surfaces of the filled vulcanizates were rougher because of silica agglomerates. Also, it is clear that the silica filled ENR vulcanizates exhibited poor filler distribution with rubber-rich areas, indicating high filler-filler interaction (Figure 14(b)). This should lower Young's modulus and the tensile strength. Better distributions of filler particles are observed in the silanized samples in Figure 14(c) of RHA_{30}-Si69 and Figure 14(e) of S_{30}-Si69. This is attributed to the functional groups of organosilane interacting with the hydroxyl groups on silica particles and dominating the filler-filler interactions to prevent agglomeration. The RHA particles in the ENR (Figure 14(b)) are much larger than the silica particles. This lowers the mechanical properties, the crosslink density, and the reinforcement relative to the silica filler. The finer dispersion of RHA particles is observed on comparing RHA_{30}-Si69 to S_{30}-Si69. This might be due to the silica ash particles of RHA being more embedded in the rubber blend matrix. In Figure 14, it is also seen that the Si69-treated ENR-25 filled vulcanizates exhibited improved phase continuity and homogeneity at the filler-rubber interfaces. This is due to the high shear mixing that dispersed particles, while simultaneously Si69 and hydroxyl groups on RHA surfaces interacted to prevent filler reagglomeration.

4. Conclusions

The main objective of this study was to demonstrate the use of rice husk ash (RHA) as an alternative filler for natural rubber. It was found that the incorporation of RHA enhanced the curing characteristics of rubber and the mechanical properties of the vulcanizate. Furthermore, the RHA offers processing advantages over silica, because the RHA/ENR-25 vulcanizates exhibited shorter optimum cure times and lower maximum torques. Moreover, as the filler concentration increases, the tensile modulus and tensile strength slightly increased, but the elongation at break decreased due to reinforcing effects. The storage modulus was also found to increase with the loading level of RHA in the composites. This is due to the increased material stiffness. The filler surface treatment with silane coupling agent improved all of the filled vulcanizates. Polar functional groups in the rubber matrix, as well as the RHA concentration, had significant effects on the mechanical properties of RHA/ENR-25 vulcanizates. That is, the polar functional groups combined with finely structured silica ash promoted crosslink density, degree of reinforcement, and mechanical strength. Moreover, the *in situ* silanization with Si69 increased the storage modulus and the loss modulus and decreased the loss tangent ($\tan \delta$), due to increased crosslinking and strong filler-rubber interactions. Also, morphological studies indicated that the reinforcement trends observed matched filler dispersion in the rubber matrix, affected by the chemical interactions between ethoxy groups of Si69 and ENR. Temperature scanning stress relaxation (TSSR) was used to investigate the relaxation behavior of materials as a function of temperature. It was found that the metal oxides in RHA promoted the degradation and deterioration of the ENR networks. Furthermore, the silanization of RHA also resulted in chemical linkages between polymer segments and the RHA particles. However, we found higher reinforcement of ENR-25 vulcanizates with silica and Si69 than with RHA and Si69. This is because of the small particle size and high specific surface area of silica and the functional Si–OH groups on silica surfaces. Nevertheless, the rice husk ash (RHA) has great potential for use as reinforcement in rubber composites, improving mechanical and other related properties.

Conflict of Interests

The authors declare that there is no conflict of interests regarding the publication of this paper.

Acknowledgments

The authors gratefully acknowledge the Thailand Research Fund (TRF) through the Royal Golden Jubilee Ph.D. Program (Grant no. PHD/0054/2553) and the Project Based Personnel Exchange Programme (PPP 2012) of the German Academic Exchange Service (DAAD) and TRF for their financial support. They are also thankful for the kind support of University of Applied Science, Osnabrück, Germany, for use of research facilities and the other support.

References

[1] C. S. L. Baker and I. R. Gelling, "Epoxidized natural rubber—a new synthetic polymer?" *Rubber World*, vol. 191, no. 6, pp. 15–20, 1985.

[2] Food and Agriculture Organization of the United Nations, *Rice Market Monitor*, vol. 16, Food and Agriculture Organization of the United Nations, 2013.

[3] Q. Zhao, B. Zhang, H. Quan, R. C. M. Yam, R. K. K. Yuen, and R. K. Y. Li, "Flame retardancy of rice husk-filled high-density polyethylene ecocomposites," *Composites Science and Technology*, vol. 69, pp. 2675–2681, 2009.

[4] H.-S. Kim, S. Kim, H.-J. Kim, and H.-S. Yang, "Thermal properties of bio-flour-filled polyolefin composites with different compatibilizing agent type and content," *Thermochimica Acta*, vol. 451, no. 1-2, pp. 181–188, 2006.

[5] H. G. B. Premalal, H. Ismail, and A. Baharin, "Comparison of the mechanical properties of rice husk powder filled polypropylene composites with talc filled polypropylene composites," *Polymer Testing*, vol. 21, no. 7, pp. 833–839, 2002.

[6] A. I. Khalf and A. A. Ward, "Use of rice husks as potential filler in styrene butadiene rubber/linear low density polyethylene blends in the presence of maleic anhydride," *Materials and Design*, vol. 31, no. 5, pp. 2414–2421, 2010.

[7] H. D. Rozman, Y. S. Yeo, G. S. Tay, and A. Abubakar, "The mechanical and physical properties of polyurethane composites based on rice husk and polyethylene glycol," *Polymer Testing*, vol. 22, no. 6, pp. 617–623, 2003.

[8] S. Siriwardena, H. Ismail, and U. S. Ishiaku, "A comparison of white rice husk ash and silica as fillers in ethylene-propylene-diene terpolymer vulcanizates," *Polymer International*, vol. 50, no. 6, pp. 707–713, 2001.

[9] W. Arayapranee and G. L. Rempel, "A comparative study of the cure characteristics, processability, mechanical properties, ageing, and morphology of rice husk ash, silica and carbon black filled 75: 25 NR/EPDM blends," *Journal of Applied Polymer Science*, vol. 109, no. 2, pp. 932–941, 2008.

[10] W. Arayapranee, N. Naranong, and G. L. Rempel, "Application of rice husk ash as fillers in the natural rubber industry," *Journal of Applied Polymer Science*, vol. 98, no. 1, pp. 34–41, 2005.

[11] Z. A. M. Ishak and A. A. Bakar, "An investigation on the potential of rice husk ash as fillers for epoxidized natural rubber (ENR)," *European Polymer Journal*, vol. 31, no. 3, pp. 259–269, 1995.

[12] S. Attharangsan, H. Ismail, M. A. Bakar, and J. Ismail, "The effect of rice husk powder on standard Malaysian natural rubber grade L (SMR L) and epoxidized natural rubber (ENR 50) composites," *Polymer-Plastics Technology and Engineering*, vol. 51, no. 3, pp. 231–237, 2012.

[13] P. Sae-Oui, C. Rakdee, and P. Thanmathorn, "Use of rice husk ash as filler in natural rubber vulcanizates: in comparison with other commercial fillers," *Journal of Applied Polymer Science*, vol. 83, no. 11, pp. 2485–2493, 2002.

[14] H. M. Da Costa, L. L. Y. Visconte, R. C. R. Nunes, and C. R. G. Furtado, "The effect of coupling agent and chemical treatment on rice husk ash- filled natural rubber composites," *Journal of Applied Polymer Science*, vol. 76, no. 7, pp. 1019–1027, 2000.

[15] D. Derouet, P. Intharapat, Q. N. Tran, F. Gohier, and C. Nakason, "Graft copolymers of natural rubber and poly(dimethyl(acryloyloxymethyl)phosphonate) (NR-g-PDMAMP) or poly(dimethyl(methacryloyloxyethyl)phosphonate) (NR-g-PDMMEP) from photopolymerization in latex medium," *European Polymer Journal*, vol. 45, no. 3, pp. 820–836, 2009.

[16] V. P. Della, I. Kühn, and D. Hotza, "Rice husk ash as an alternate source for active silica production," *Materials Letters*, vol. 57, pp. 818–821, 2002.

[17] L. Guy, S. Daudey, P. Cochet, and Y. Bomal, "New insights in the dynamic properties of precipitated silica filled rubber using a new high surface silica," *Kautschuk Gummi Kunststoffe*, vol. 62, no. 7-8, pp. 383–391, 2009.

[18] S. Thongsang and N. Sombatsompop, "Dynamic rebound behavior of silica/natural rubber composites: fly ash particles and precipitated silica," *Journal of Macromolecular Science, Part B: Physics*, vol. 46, no. 4, pp. 825–840, 2007.

[19] P. J. Flory and J. Rehner Jr., "Statistical mechanics of cross-linked polymer networks II. Swelling," *The Journal of Chemical Physics*, vol. 11, no. 11, pp. 521–526, 1943.

[20] P. J. Flory, "Molecular size distribution in three dimensional polymers. II. Trifunctional branching units," *Journal of the American Chemical Society*, vol. 63, no. 11, pp. 3091–3096, 1941.

[21] N. Vennemann, K. Bökamp, and D. Bröker, "Crosslink density of peroxide cured TPV," *Macromolecular Symposia*, vol. 245-246, pp. 641–650, 2006.

[22] N. Vennemann, M. Wu, and M. Heinz, "Thermoelastic properties and relaxation behavior of S-SBR/silica vulcanizates," *Rubber World*, vol. 246, no. 6, pp. 18–23, 2012.

[23] N. Vennemann, *Characterization of Thermoplastic Elastomers by Means of Temperature Scanning Stress Relaxation Measurements, Thermoplastic Elastomers*, A. El-Sonbati, Ed., InTech, Rijeka, Croatia, 2012.

[24] J. Kruželák, C. Kyselá, and I. Hudec, "Elastomeric magnetic composites—curing and properties," *Kautschuk Gummi Kunststoffe*, vol. 61, no. 9, pp. 424–428, 2008.

[25] B. T. Poh, C. P. Kwok, and G. H. Lim, "Reversion behaviour of epoxidized natural rubber," *European Polymer Journal*, vol. 31, no. 3, pp. 223–226, 1995.

[26] M. P. Wagner, "Reinforcing silicas and silicates," *Rubber Chemistry and Technology*, vol. 49, no. 3, pp. 703–774, 1976.

[27] H. M. da Costa, L. L. Y. Visconte, R. C. R. Nunes, and C. R. G. Furtado, "Rice husk ash filled natural rubber. III. Role of metal oxides in kinetics of sulfur vulcanization," *Journal of Applied Polymer Science*, vol. 90, no. 6, pp. 1519–1531, 2003.

[28] A. S. Hashim, B. Azahari, Y. Ikeda, and S. Kohjiya, "The effect of bis(3-triethoxysilylpropyl) tetrasulfide on silica reinforcement of styrene-butadiene rubber," *Rubber Chemistry and Technology*, vol. 71, no. 2, pp. 289–299, 1998.

[29] S. Thongsang, W. Vorakhan, E. Wimolmala, and N. Sombatsompop, "Dynamic mechanical analysis and tribological properties of NR vulcanizates with fly ash/precipitated silica hybrid filler," *Tribology International*, vol. 53, pp. 134–141, 2012.

[30] M. Jacob, B. Francis, S. Thomas, and K. T. Varughese, "Dynamical mechanical analysis of sisal/oil palm hybrid fiber-reinforced natural rubber composites," *Polymer Composites*, vol. 27, no. 6, pp. 671–680, 2006.

[31] Y. Y. Luo, Y. Q. Wang, J. P. Zhong, C. Z. He, Y. Z. Li, and Z. Peng, "Interaction between fumed-silica and epoxidized natural rubber," *Journal of Inorganic and Organometallic Polymers and Materials*, vol. 21, no. 4, pp. 777–783, 2011.

[32] A. K. Manna, P. P. de, D. K. Tripathy, S. K. de, and D. G. Peiffer, "Bonding between precipitated silica and epoxidized natural rubber in the presence of silane coupling agent," *Journal of Applied Polymer Science*, vol. 74, no. 2, pp. 389–398, 1999.

[33] W. Keawsakul, K. Sahakaro, W. K. Dierkes, and J. W. M. Noordermeer, "Optimization of mixing conditions for silica-reinforced natural rubber tire tread compounds," *Rubber Chemistry and Technology*, vol. 201, pp. 277–294, 2012.

[34] S. Pichaiyut, C. Nakason, C. Kummerlöwe, and N. Vennemann, "Thermoplastic elastomer based on epoxidized natural rubber/thermoplastic polyurethane blends: influence of blending technique," *Polymers for Advanced Technologies*, vol. 23, no. 6, pp. 1011–1019, 2012.

[35] N. Vennemann, C. Schwarze, and C. Kummerlöwe, "Determination of crosslink density and network structure of NR vulcanizates by means of TSSR," *Advanced Materials Research*, vol. 844, pp. 482–485, 2013.